Supporting Information

NCQDs-Induced Nitrogen Configuration Engineering Construct Hybrid CN with Exceptionally High Nitrogen-Content and Predominantly Pyrrolic/Pyridinic-N for Catalytic Hydrogenation

Chaofan Ma[1], Xiaotian Xu[1], Miaoqi Xu[1], Yebin Zhou[1], Yongyue Yao[1], Zhenli Xiang[1], Wei He[1], Jiaxin Yu[1], Qunfeng Zhang[1], Feng Feng[1], Yi Liu[1], Chunyu Yin[1], Xiaonian Li[1*], Chunshan Lu[1,2*]*

1. State Key Laboratory Breeding Base of Green Chemistry Synthesis Technology, Zhejiang University of Technology, Hangzhou 310032, People's Republic of China.

2. The Baima Lake Laboratory, Hangzhou 310051, People's Republic of China.

E-mail: cyyiny@zjut.edu.cn;

xnli@zjut.edu.cn;

lcszjcn@zjut.edu.cn;

Number of pages: 40

Number of figures: 25

Number of tables: 5

Table of Contents

1. Experimental Section

1.1 Materials

Chloroplatinic Acid (H_2PtCl_6) (GR), ethylenediamine (EDA) (GC) were purchased from Aladdin Chemistry Co. Ltd. (Shanghai, China). Citric acid monohydrate (CA) (AR) was purchased from Sinopharm Chemical Reagent Co., Ltd. (Shanghai, China). Dicyandiamide (AR) and methanol (AR) were bought from Shanghai Lingfeng Chemical Reagent Co., Ltd. (Shanghai, China). All the chemicals were used directly without another purification treatment.

1.2 Synthesis of NCQDs

CA and EDA were used as carbon source and nitrogen dopant respectively to synthesize the NCQDs via a common microwave pyrolysis method. Typically, 20 g CA and 3 mL EDA were dissolved in 100 mL deionized water, then heated in a domestic microwave oven (Midea, M1-211A) for 10 min under the power of 700 W. After cooling to room temperature, the crude product was mixed with 75 mL deionized water, then filtered through a 0.22 μm membrane filter to remove the large particles. The filtered solution was further dialyzed using a membrane of MWCO of 1 kD for 12 h against deionized water. Finally, a pure and yellow NCQDs was obtained by lyophilizing.

1.3 Preparation of the Catalysts

1.3.1 Preparation of the Pt/NCQDs$_x$/CN

A facile thermal polymerization was used to synthesize NCQDs modified hybrid nitride carbon. First, 20 g NCQDs solid was dissolved in

100 mL deionized water to make a solution with 20 wt.% NCQDs. After that, 5 g dicyandiamide was dissolved in 20 mL solution which contains x mL NCQDs (x = 0,3,5,10,20 mL), keeping stirring for 3 h. The resultant solution was dried at 90 °C to collect light yellow powder, labeled as NCQDs-DICY. Finally, the dark hybrid nitride carbon support mixed with different content of NCQDs, denoted as $NCQDs_x$/CN, was obtained by calcining the precursor powder under nitrogen atmosphere at 550 °C for 3 h with a heating rate of 2.8 °C·min^{-1}. The pristine CN was prepared by the same process without the addition of NCQDs, and thus is consistent with $NCQDs_0$/CN.

In addition, 10 mL NCQDs (20 wt.%) was dried at 90 °C to collect light yellow powder, and the powder was calcined under nitrogen atmosphere at 550 °C for 3 h with a heating rate of 2.8 °C·min^{-1}, the product was named as $NCQDs_{cal}$. After that, the $NCQDs_{cal}$ and 5 g dicyandiamide were added to 20 mL deionized water, keeping stirring for 3 h. The resultant solution was dried at 90 °C to obtain a powder labeled as $NCQDs_{cal}$-DICY, the obtained product was calcined at 550 °C for 3 h with a heating rate of 2.8 °C·min^{-1} in a tube furnace with nitrogen atmosphere to synthesis $NCQDs_{cal}$/CN.

After that, 0.5 g $NCQDs_x$/CN and 1.0 mL chloroplatinic acid solution (0.0086 g/mL) were added to 85 mL deionized water. After stirring for 3 h, the solution was transferred into a Teflon lined stainless hydrothermal reactor and heated for 10 h at 180 °C. The products were dried under 70 °C for 3 h in a vacuum oven, labeled as Pt/$NCQDs_x$/CN.

1.3.2 Preparation of the Pt/NCQDs and Pt/NCQDs-CN

0.5 g product, obtained by the calcination of 2 g NCQDs at 550 °C under N_2 for 3 h with a heating rate of 2.8 °C·min^{-1}, and 1.0 mL

chloroplatinic acid solution (0.0086 g/mL) were added to 85 mL deionized water. After stirring for 8 h, the solution was transferred into a Teflon lined stainless hydrothermal reactor and heated for 10 h at 180 ℃. The products were dried under 70 ℃ for 3 h in a vacuum oven, labeled as Pt/NCQDs.

For Pt/NCQDs-CN, 0.5 g product, obtained by the calcination of 2 g NCQDs at 550 °C for 3 h with a heating rate of 2.8 °C·min^{-1}, was physically mixed pristine CN at a ratio of 1:1 to prepare NCQDs-CN. The process of metal growth was the same as above, while the carbon support is replaced with NCQDs-CN.

1.3.3 Preparation of the Pt/CN-RM

To clarify the necessity of NCQDs rather than small molecules in catalysis, mixed equal amount raw materials of $NCQDs_{10}$/CN to prepare the precursor of CN-RM. Specifically, 4 g CA, 0.6 mL EDA and 5 g dicyandiamide were dissolved in 20 mL deionized water and evaporated at 90 °C after homogenized. After that, the product was heated to 550 °C at a heating rate of 2.8 °C·min^{-1} and kept for 3 h under nitrogen atmosphere. Meanwhile, replaced $NCQDs_x$/CN with CN-RM and kept other steps consistent to prepare Pt/CN-RM.

1.4 Characterization

The TEM images were obtained by a transmission electron microscope (JEM-F200, 300 kV), while the features and morphologies were performed via scanning electron microscopy (SEM, SU8100). To prove the well UV−vis response of NCQDs, the UV−vis absorption spectrum of NCQDs was studied via a GENESY 150 Spectrophotometer of ThermoFisher, however, the UV-vis diffuse reflectance spectra of catalysts were collected by UV-2600i of Shimadzu. The crystal structures of catalysts were

analyzed on a ThermoFisher ARL SCINTAG XTRA X-ray powder diffractometer using a Cu Kα radiation source at 45 kV and 40 mA. The functional groups of samples were carried out by Nicolet 6700 FT-IR spectrometer with KBr pellets. The Brunauer–Emmett–Teller (BET) specific surface and porous parameters of catalysts were performed by N_2 adsorption-desorption on a Micromeritics ASAP 2020 instrument. The defect degree of catalysts was detected by Raman on Horiba LabRAM Odyssey equipped with a laser of 532 nm. X-ray photoelectron spectroscopy (XPS) and Ultraviolet photoelectron spectroscopy (UPS) were recorded on Thermo Scientific ESCALAB 250Xi with monochromatized aluminum X-ray source (1486.6 eV) using the C 1s peak at 284.8 eV as a standard to correct the other peaks. The samples were purged with dry Ar (50 mL/min, purity> 99.999%) at 120 °C for 2.0 h to remove the adsorbed water, and then the H_2-TPR-MS was performed in the range of 50~800 °C at a rate of 10 °C/min during the H_2/Ar atmosphere. The captured mass signals were characterized according to the mass-charge on a quadrupole mass spectrometer. The PL emission spectra were performed with 375 nm light source at Edinburgh FLS1000. The actual Pt content in the sample was analyzed using the air-acetylene flame atomic absorption spectrophotometer (AAS) on a Beijing Purkinje TAS-990 atomic absorption spectrophotometer.

1.5 Computational methods

The DFT models and computations were constructed and performed through the Materials Studio software. The exchange dependent functional were described by the functional Perdew-Burke-Ernzerhof (PBE) generalized gradient approximation (GGA). The plane-wave cut-off energy was set as 400 eV. The SCF tolerance of 1×10^{-6} eV/atom was used

to calculate the total energy and the electron to obtain well-converged convergent geometry. The sampling of the Brillioun zone was done using a 2×2×2 k-points for geometry optimizations and the projected density of states (PDOS) calculations. All the models were built a periodic supercell containing a vacuum of 15 Å in the z-direction. In addition, the adsorption energy (E_{ads}) is obtained by the formula: $E_{ads} = E_{adsorbate/substrate} - (E_{adsorbate} + E_{substrate})$

1.6 Formula description

Formula 1:

$$at.\% = \left(\frac{wt.\%/M_A}{wt.\%/M_A + (100 - wt.\%)/_{MB}}\right) \times 100$$

at. %: This term refers to the percentage of atoms of a specific element relative to the total number of atoms in a material;

wt. %: This term refers to the percentage of the mass of a specific element relative to the total mass of the material;

M_A: the atomic weights of element A;

M_B: the atomic weights of element B.

Formula 2:

$$(\alpha h\upsilon)^{1/n} = B(h\upsilon - E_g)$$

α: the absorption coefficient;

hυ: the photon energy;

h: Planck's constant, is around $4.13567*10^{-15}$eV·s;

υ: the photon frequency, $\upsilon = \frac{c}{\lambda}$, where c is the speed of light, λ is the wavelength of the incident light;

B: the proportionality constant;

E_g: the band gap width of the semiconductor material;

The value of n is related to the type of semiconductor material, when the semiconductor material is a direct band gap, n=1/2; When the semiconductor material is an indirect band gap, n=2.

Formula 3:

$$E_{VB} = E_{CB} + E_g$$

E_{VB}: the valence band value of semiconductor material;

E_{CB}: the conduction band value of semiconductor material;
E_g: the band gap width of the semiconductor material.

Formula 4:

$$\Phi = h\upsilon - E_{cutoff}$$

Φ: the work function;
hυ: the photon energy;
h: Planck's constant, is around $4.13567*10^{-15}$eV·s;

υ: the photon frequency, $\upsilon = \frac{c}{\lambda}$, where c is the speed of light, λ is the wavelength of the incident light;

Ecutoff: the cutoff energy, which threshold required for electrons to escape from the surface of a solid (usually a metal).

2. Supplementary Figures

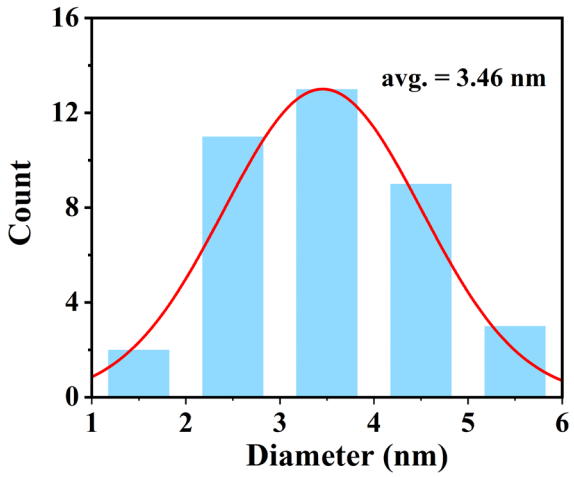

Fig. S1 Particle size distribution of NCQDs.

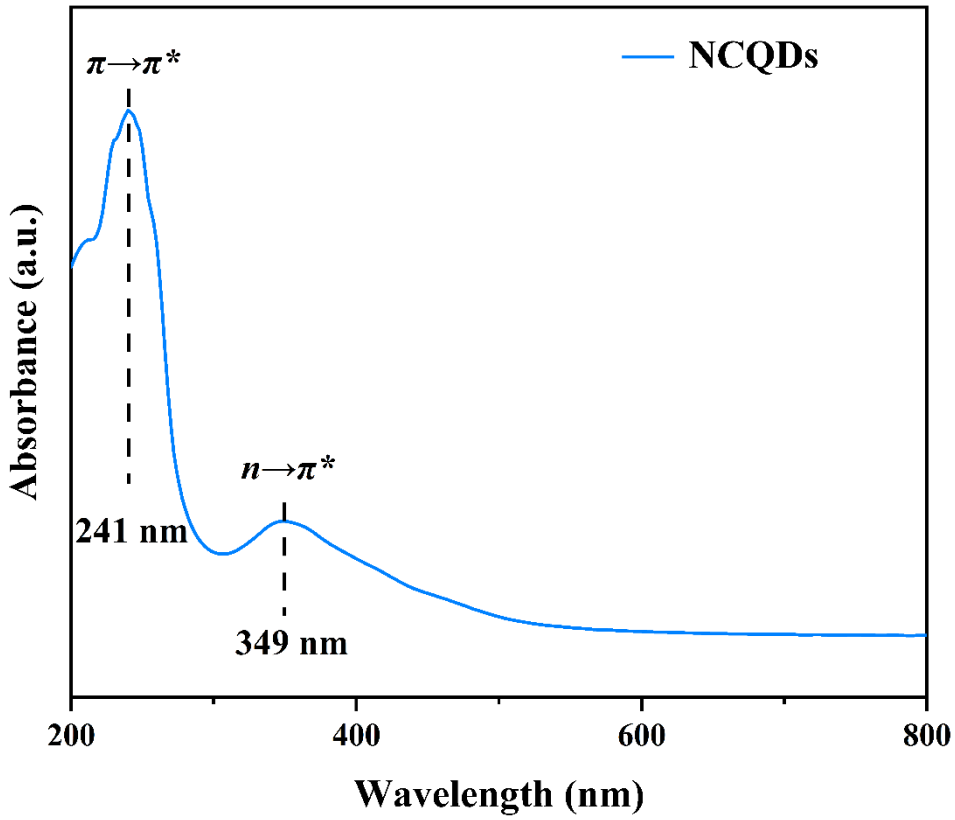

Fig. S2 The UV-vis absorption spectrum of NCQDs.

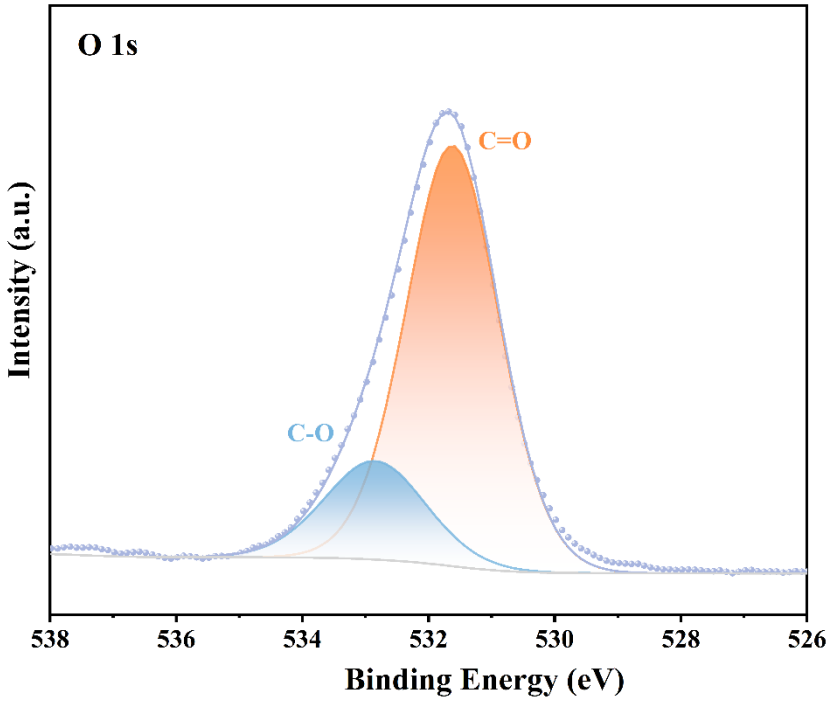

Fig. S3 The O 1s XPS spectrum of NCQDs.

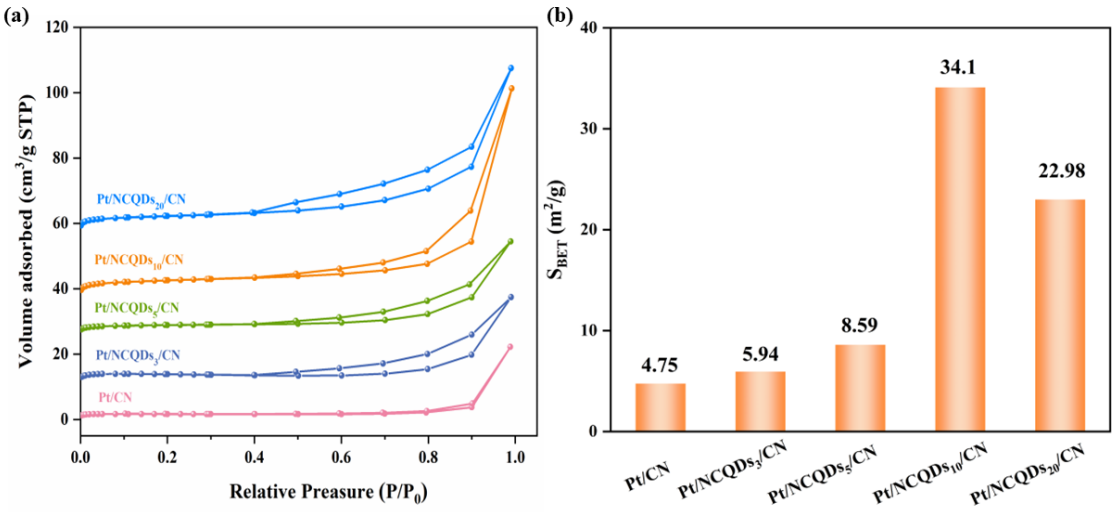

Fig. S4 (a) N_2 adsorption−desorption isotherms and (b) calculated surface areas of Pt/NCQDs$_x$/CN.

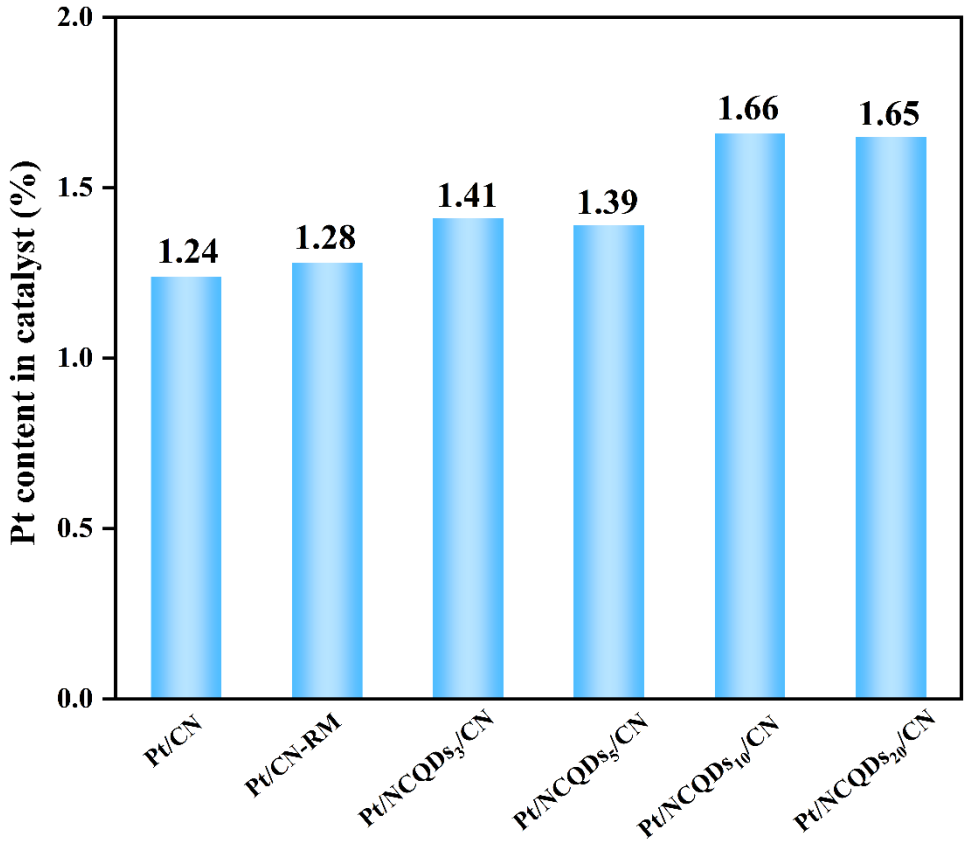

Fig. S5 The loading content of Pt in catalysts calculated by AAS.

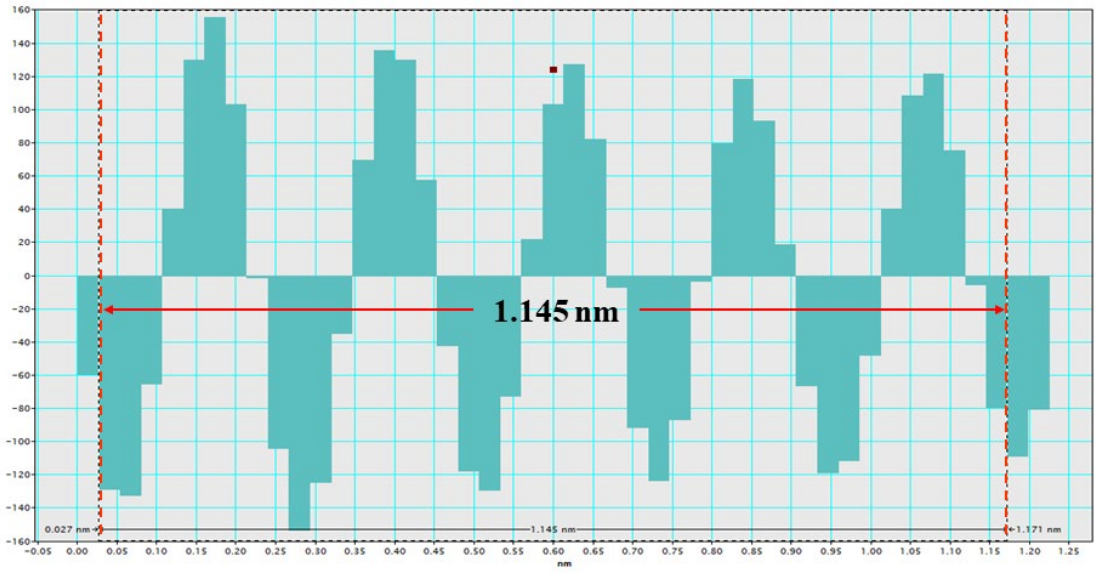

Fig. S6 The inverse FFT profile for calculating lattice fringe spacing of (a) Pt (111) based on HRTEM of Pt/NCQDs$_{10}$/CN.

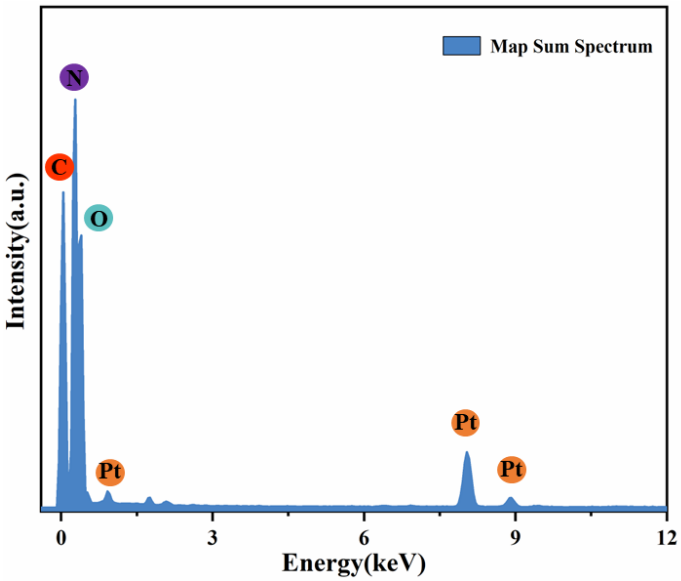

Fig. S7 The energy-dispersive spectrometer (EDS) spectrum of Pt/NCQDs$_{10}$/CN.

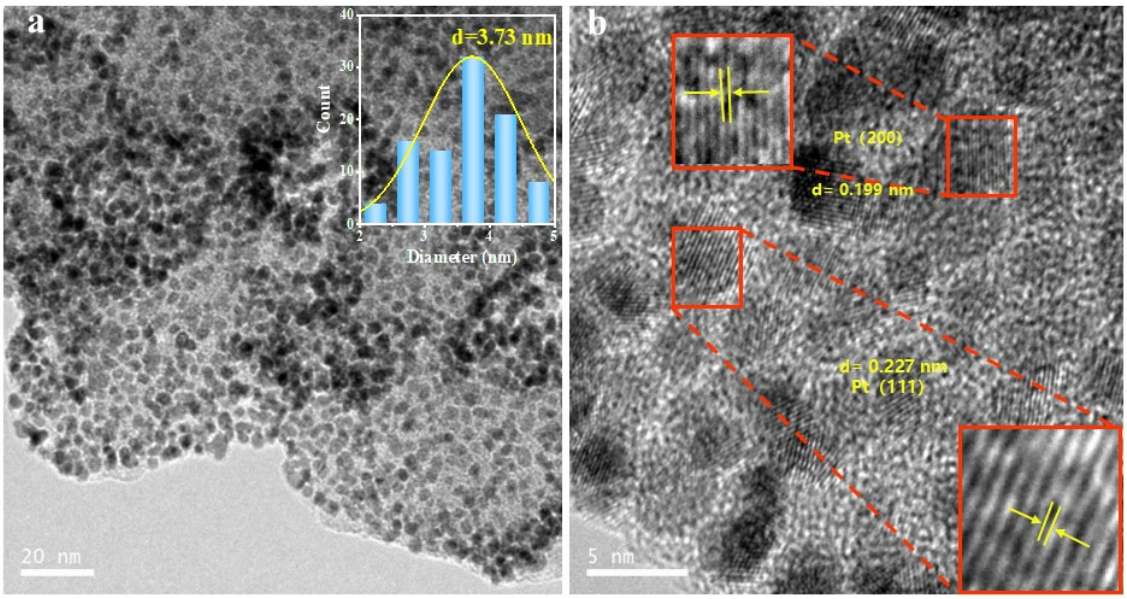

Fig. S8 The TEM images and metal particle size distribution (inset) of Pt/NCQDs$_{20}$/CN.

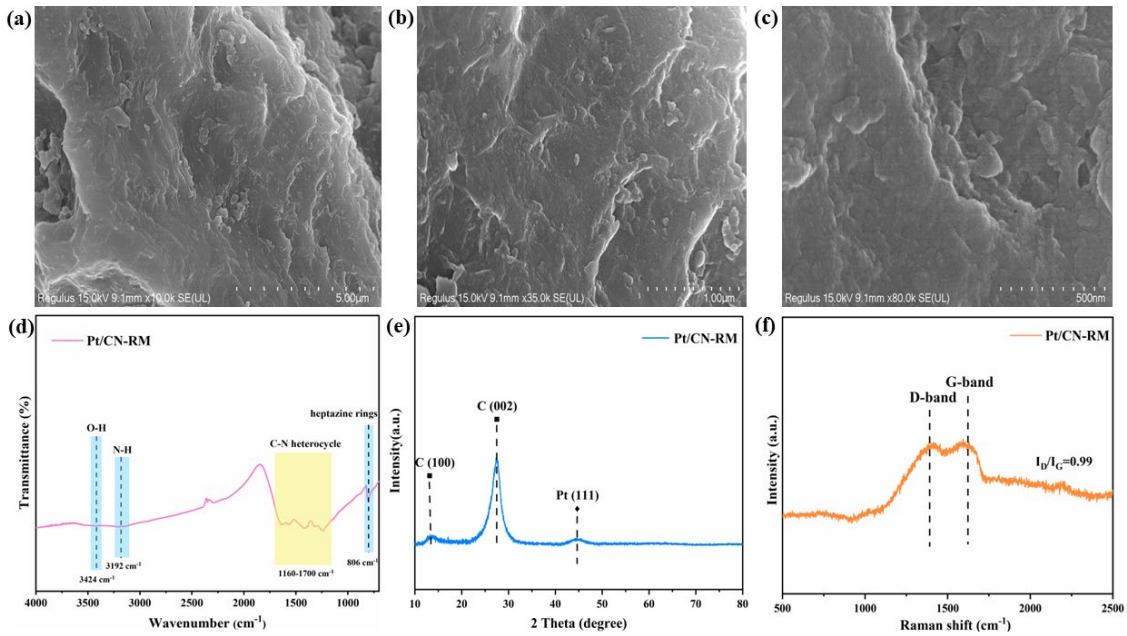

Fig. S9 (a-c) SEM images, (d)FT-IR spectrum, (e) XRD pattern and (f) Raman spectrum of Pt/CN-RM.

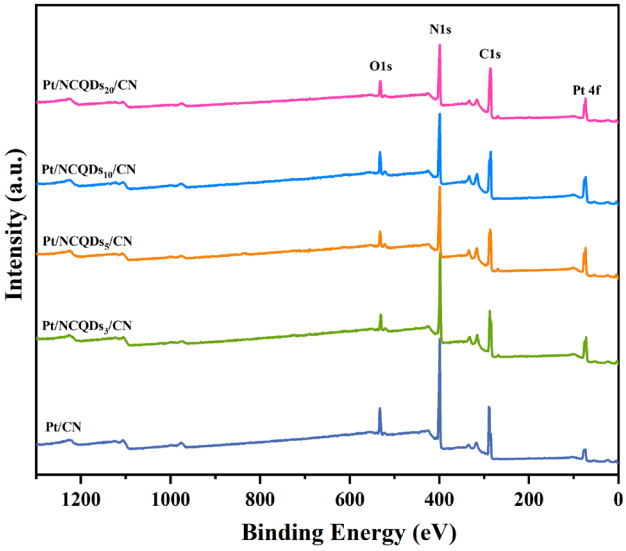

Fig. S10 The XPS survey spectra of Pt/NCQDs$_x$/CN.

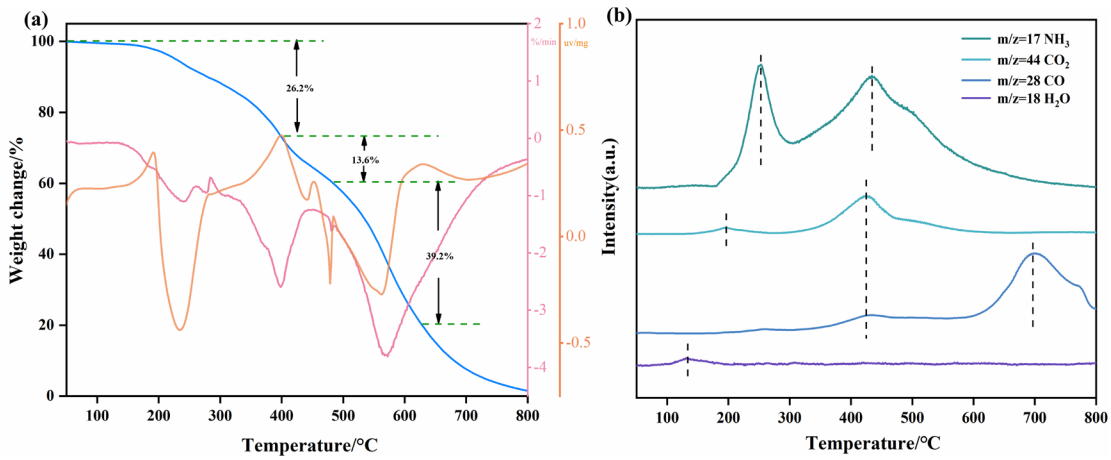

Fig. S11 (a) TGA pattern and (b) corresponding MS curves of precursor of NCQDs$_{10}$/CN measured at a ramp rate of 10 K/min.

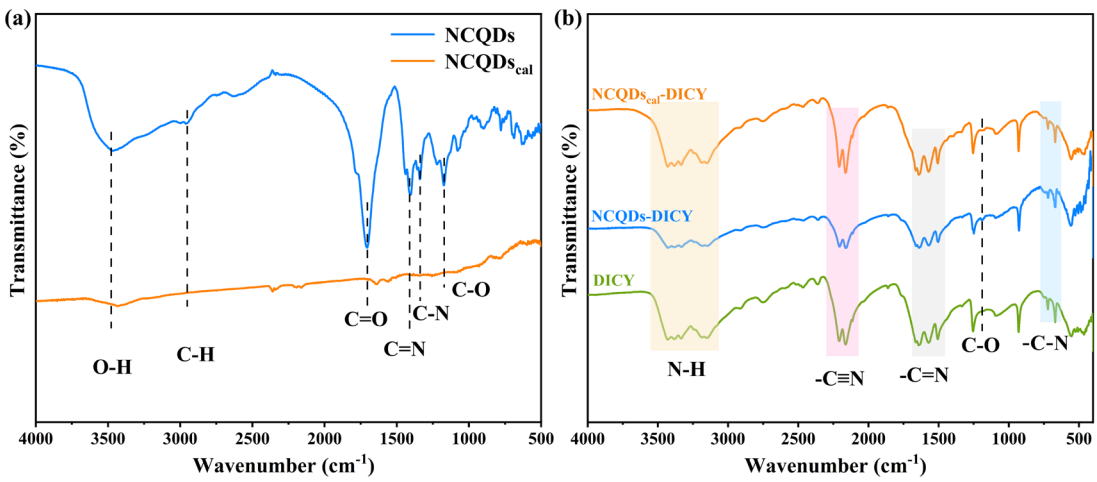

Fig. S12 The FT-IR spectra of the samples

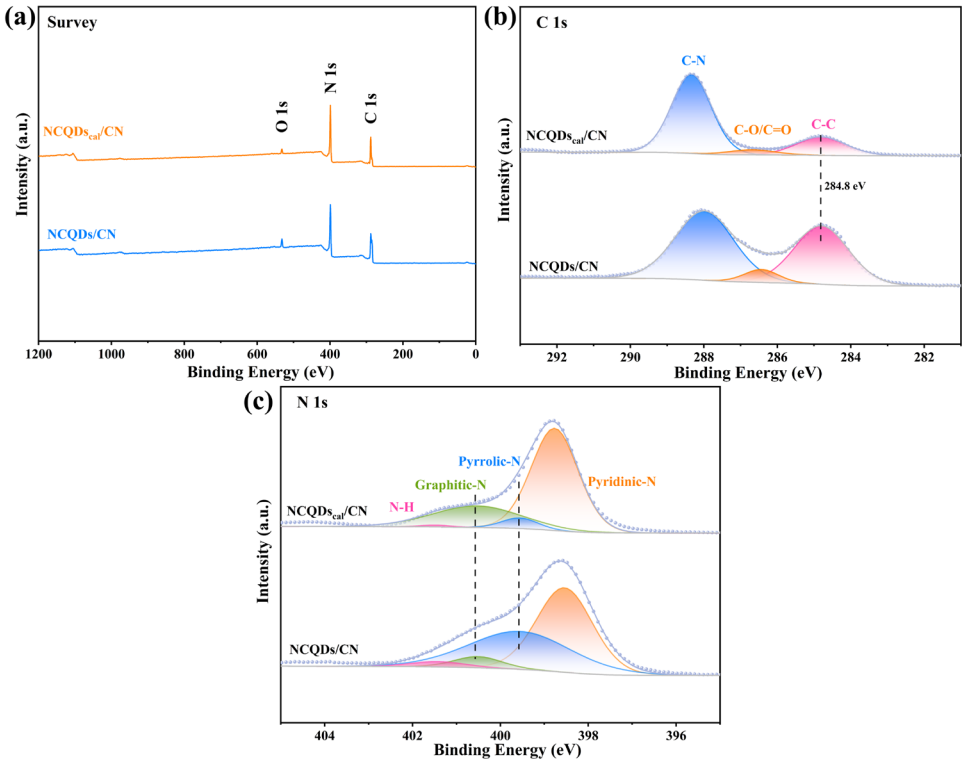

Fig. S13 (a) XPS survey spectra, (b) C 1s XPS spectra and (c) N1s XPS spectra of NCQDs/CN and NCQDs$_{cal}$/CN.

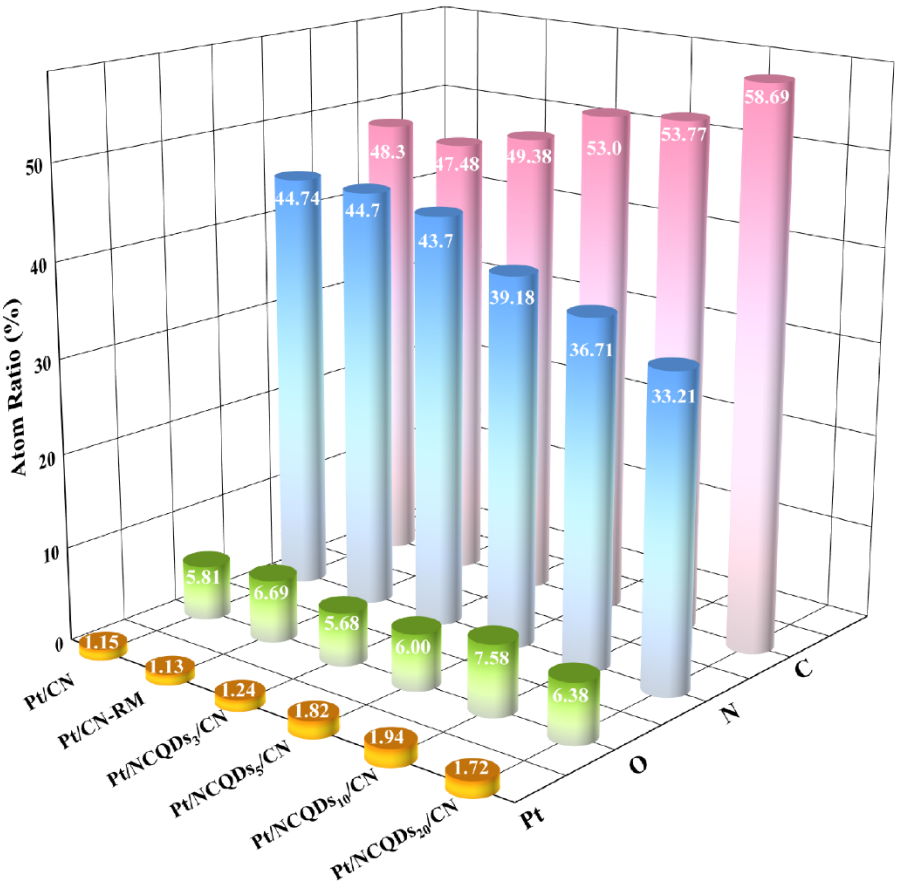

Fig. S14 Elemental contents of Pt/NCQDs$_x$/CN and Pt/CN-RM.

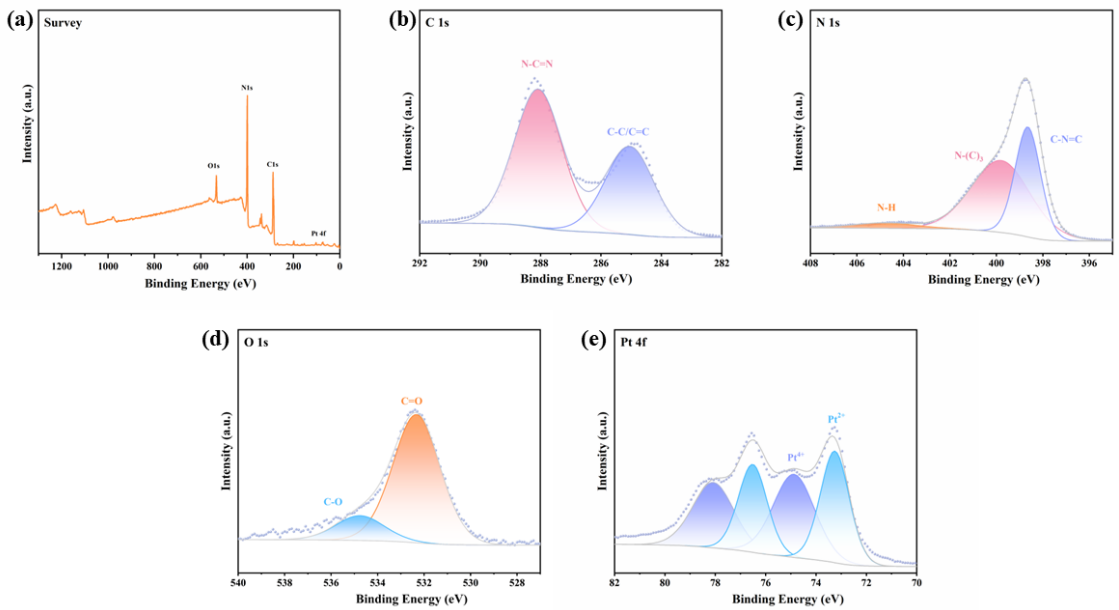

Fig. S15 (a) XPS survey spectrum, (b) C 1s spectrum, (c) N 1s spectrum, (d) O 1s spectrum and (e) Pt 4f spectrum of Pt/CN-RM.

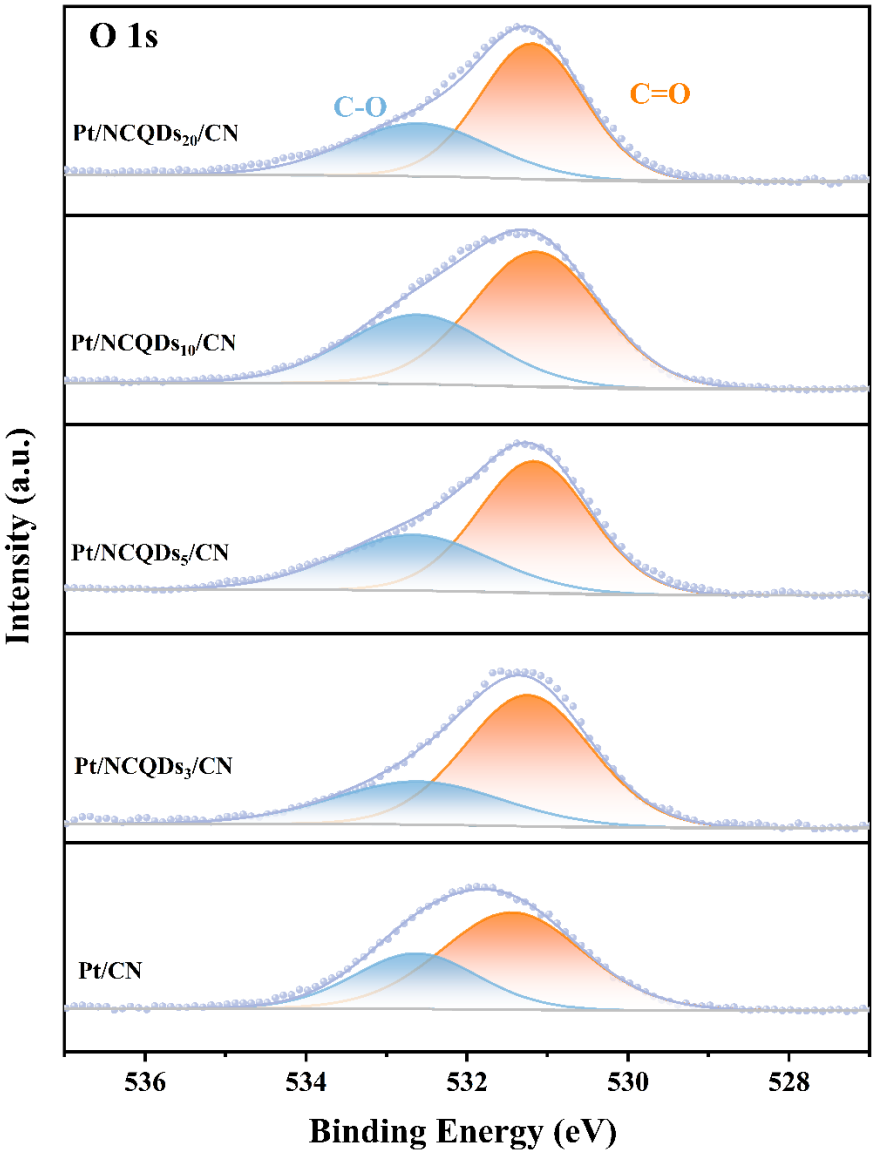

Fig. S16 The O1s XPS survey spectra of Pt/NCQDs$_x$/CN.

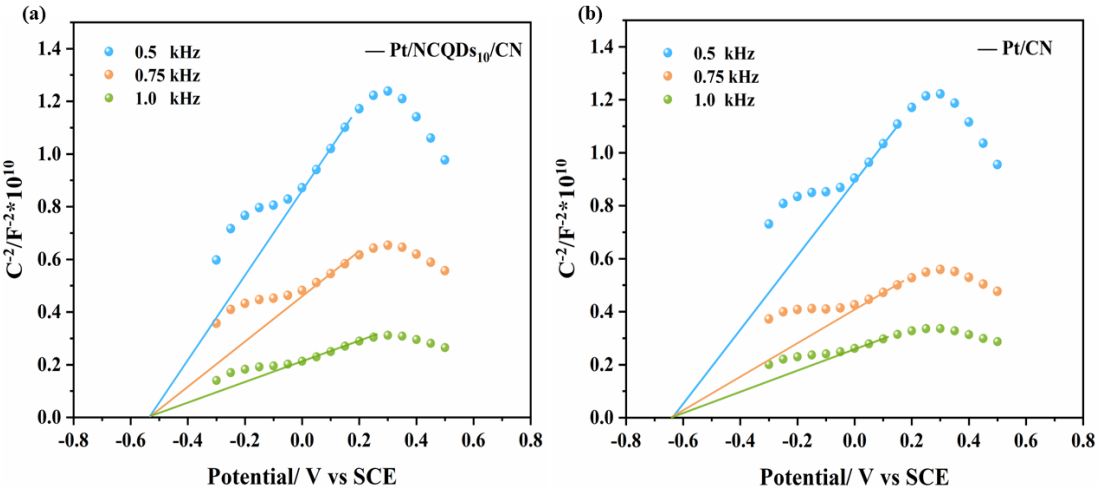

Fig. S17 The Mott-Schottky plots of (a) Pt/NCQDs$_{10}$/CN and (b) Pt/CN.

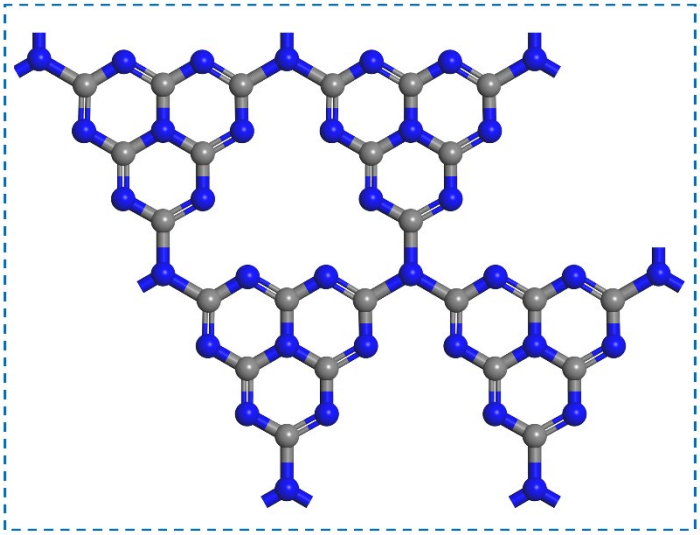

Fig. S18 Proposed configuration of CN.

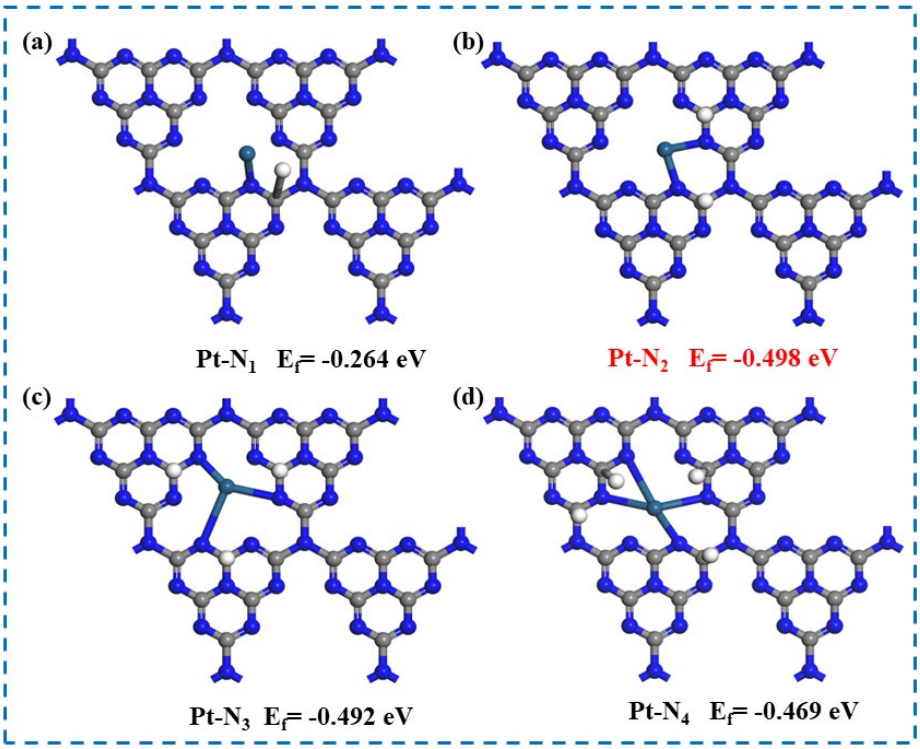

Fig. S19 Formation energies for different configurations of Pt/CN.

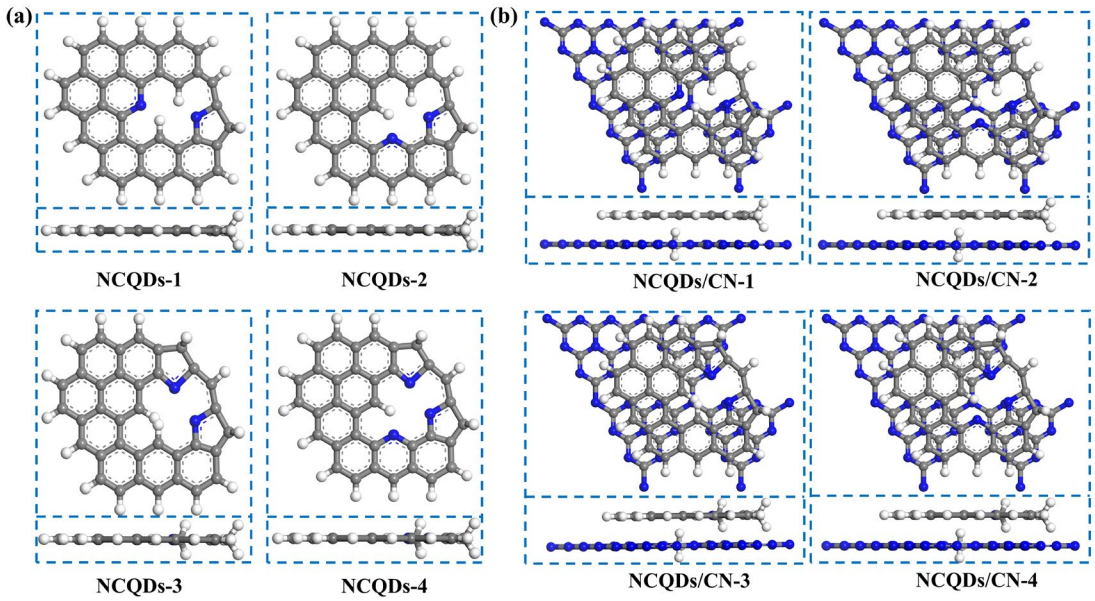

Fig. S20 Different configurations of (a) NCQDs and corresponding (b) NCQDs/CN from top view and side view.

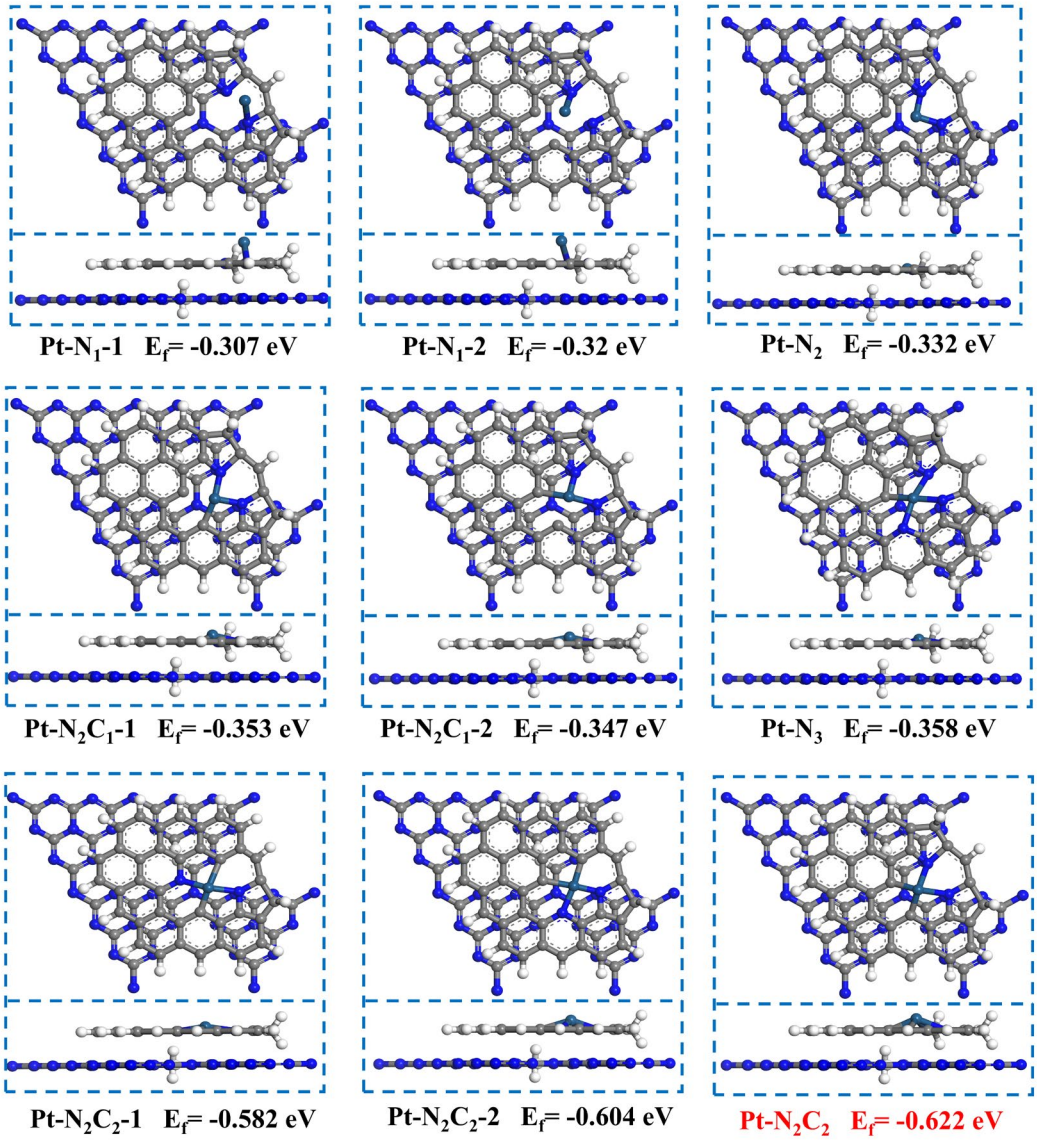

Fig. S21 Formation energies for different configurations of Pt/NCQDs$_{10}$/CN.

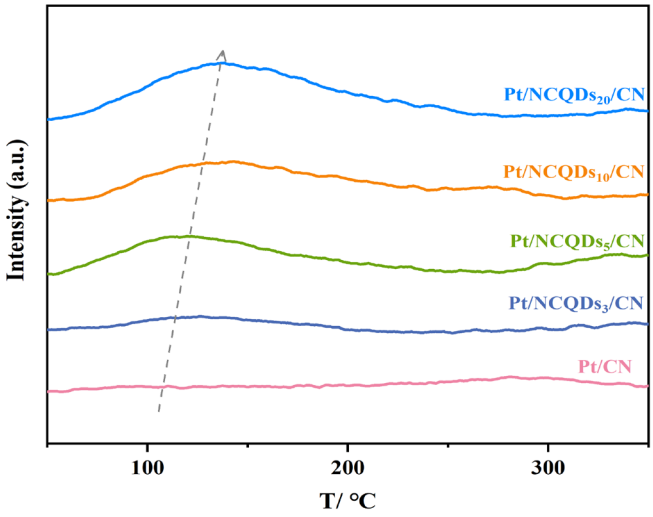

Fig. S22 The H_2-TPD profiles of Pt/NCQDs$_x$/CN.

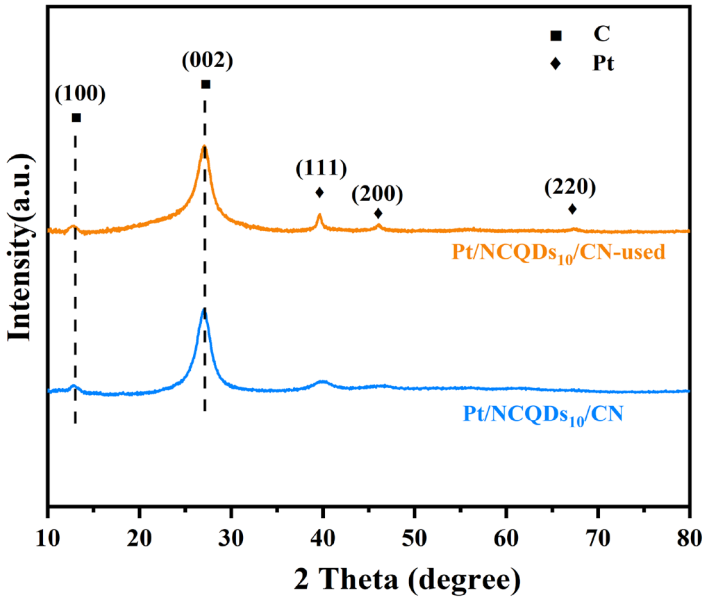

Fig. S23 The XRD pattern of used and fresh Pt/NCQDs$_{10}$/CN.

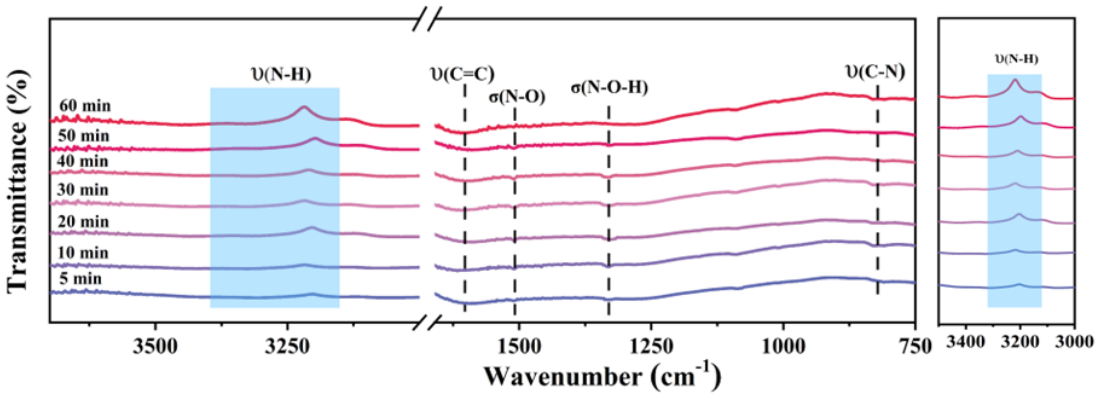

Fig. S24 The *in situ* FT-IR spectra for the hydrogenation reaction of *p*-CNB over Pt/NCQDs$_{10}$/CN for 60 min.

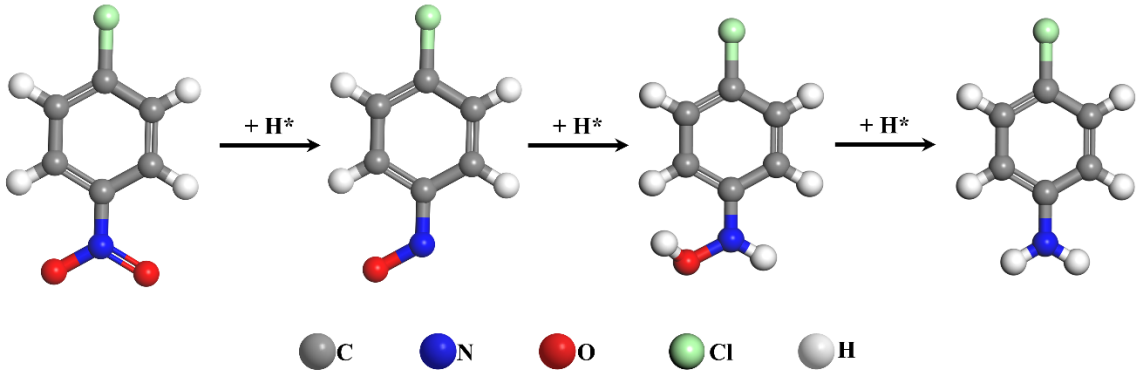

Fig. S25 The possible catalytic hydrogenation route of *p*-CNB on Pt/NCQDs$_{10}$/CN.

3. Supplementary Tables

Table S1. Atom and corresponding species ratio of NCQDs calculated by XPS

Atoms	Species (%)		Atom ratio
C	C-C/C=C	49.45%	62.85%
	C-N	21.48%	
	C=O/C-O	29.07%	
N	Pyridinic N	10.97%	10.65%
	Pyrrolic N	74.78%	
	Graphitic N	14.25%	
O	C=O	79.69%	26.5%
	C-O	20.31%	

Table S2. Atom and corresponding species ratio of Pt/NCQDs$_x$/CN catalysts calculated by XPS

Atoms	Species	Pt/CN (%)	Pt/NCQDs$_3$/CN (%)	Pt/NCQDs$_5$/CN (%)	Pt/NCQDs$_{10}$/CN (%)	Pt/NCQDs$_{20}$/CN (%)
C	C-C/C=C	29.24	33.18	36.8	42.14	43.33
	C-O/C=O	0	21.49	24.02	23.58	26.66
	N-C=N	70.76	45.33	39.17	34.28	30.01
N	Pyridinic N	69.59	44.63	51.48	33.62	31.76
	Pyrrolic N	0	31.34	26.76	57.28	57.16
	Graphitic N	28.98	21.99	18.53	5.96	3.64
	N-H	1.44	2.04	3.23	3.14	7.43
Pt	Pt^0	0	3.77	4.54	72.3	72.18
	Pt^{2+}	66.39	96.23	95.46	27.7	27.82
	Pt^{4+}	33.61	0	0	0	0
O	C=O	66.82	69.46	63.4	63.33	64.91
	C-O	33.18	30.54	36.6	36.67	35.19

Table S3. Binding energy of Pt/NCQDs$_x$/CN catalysts calculated by XPS

Atoms	Species	Pt/CN (eV)	Pt/NCQDs$_3$/CN (eV)	Pt/NCQDs$_5$/CN (eV)	Pt/NCQDs$_{10}$/CN (eV)	Pt/NCQDs$_{20}$/CN (eV)
C	C-C/C=C	284.8	284.8	284.82	284.83	284.83
	C-O/C=O		286.29	286.12	286.42	286.32
	N-C=N	288.08	287.85	287.85	287.95	287.83
N	Pyridinic N	398.26	398.28	398.28	398.36	398.37
	Pyrrolic N	/	398.87	399.11	399.41	399.36
	Graphitic N	399.8	400.00	400.18	400.29	400.37
	N-H	401.21	401.28	401.24	401.22	401.5
Pt	Pt^0	/	70.88/74.05	70.38/74.07	70.92/74.32	70.73/74.12
	Pt^{2+}	72.85/ 76.14	72.74/76.04	72.65/75.95	72.63/75.91	72.68/76.03
	Pt^{4+}	74.45/ 77.81	/	/	/	/
O	C=O	531.44	531.24	531.17	531.14	531.19
	C-O	532.63	532.61	532.67	532.61	532.61

Table S4. The catalytic performance of catalysts for the hydrogenation of p-CNB[a]

Entry	Catalyst	Reaction time (min)	Reaction rate[b] ($mol_{p\text{-}CNB}/h \cdot mol_{Pt}$)	Conv. (%)	Sel. (%)
1	Pt/CN	45	94.1	14.13	71.6
2	Pt/CN-RM	45	80.7	12.51	76.5
3	Pt/NCQDs	45	176.8	36.21	54.6
4	Pt/NCQDs-CN	45	166.8	34.17	64.3
5	$Pt/NCQDs_3/CN$	45	232.1	39.65	74.9
6	$Pt/NCQDs_5/CN$	45	474.6	79.92	93.7
7	$Pt/NCQDs_{10}/CN$	45	497.3	100	99.9
8	$Pt/NCQDs_{20}/CN$	45	310.2	62	84

[a] Reaction conditions: 0.01 g catalyst, 0.5 g p-CNB, 25 mL methanol, T=40 °C, 1 MPa H_2.
[b] Reaction rate: moles of converted p-CNB per mole of Pt per hour.

Table S5. Comparison of the catalytic performance for the hydrogenation of *p*-CNB to *p*-CAN in literatures.

Catalyst	w_{cat}(mg)	$n_{p\text{-}CNB}$ (mmol)	P/MPa	Reaction time (min)	Conv. (%)	Sel. (%)	Ref.
Pt/NCQDs$_{10}$/CN	10	3.17	1	45	100	99.9	This work
5%Pt/CMK-3	25	21	4	5	100	56.8	[1]
Pt/MIL-101	50	21	4	10	99.8	77.3	[2]
3%Pt/CeO_2	23.9 mg Pt	0.8	1	15	99.1	86.9	[3]
Pt_2/mpg-C_3N_4	0.07 mg Pt	1	1	180	99	93	[4]
Pd@Pt-1/1/Al_2O_3	100	12.6	0.1	180	88	86.9	[5]
Pt–NiO@mSiO_2	179	3.8	1 atm	120	87.9	95.3	[6]
Pt/NiO/Al_2O_3	200	63	3	120	79.8	89.91	[7]
Pt/$Ti_3C_2T_x$-AB	5	1	1	60	70.3	89.9	[8]
PVP–La–Pt	1.1 mg Pt	4	0.1	725	63	72.3	[9]
PtCu/CNTs	150	4	0.1	240	57.4	92.3	[10]
$Pt_{0.0002}$–$Au_{0.005}$/TiO_2	25	2.5	1	30	55.2	97.3	[11]
$Pt_{0.9}$/SMC	10	0.5	1 atm	150	51.6	70.5	[12]
Pt/SiO_2	10	0.6	0.1	60	40.4	55.2	[13]
0.3% Pt/AC	20	6.3	1	40	37	83	[14]
Pt(1.10%)/TAPT-COF	10	0.5	H_2 balloon	180	36.6	94.4	[15]

Reference

1. Li, J.; Li, X.; Ding, Y.; Wu, P., Pt nanoparticles entrapped in ordered mesoporous carbons: An efficient catalyst for the liquid-phase hydrogenation of nitrobenzene and its derivatives. *Chinese Journal of Catalysis* **2015,** *36* (11), 1995-2003.

2. Pan, H.; Li, X.; Yu, Y.; Li, J.; Hu, J.; Guan, Y.; Wu, P., Pt nanoparticles entrapped in mesoporous metal-organic frameworks MIL-101 as an efficient catalyst for liquid-phase hydrogenation of benzaldehydes and nitrobenzenes. *J Mol Catal a-Chem* **2015,** *399*, 1-9.

3. Wang, C.; Mao, S.; Wang, Z.; Chen, Y.; Yuan, W.; Ou, Y.; Zhang, H.; Gong, Y.; Wang, Y.; Mei, B.; Jiang, Z.; Wang, Y., Insight into Single-Atom-Induced Unconventional Size Dependence over CeO_2-Supported Pt Catalysts. *Chem-Us* **2020,** *6* (3), 752-765.

4. Tian, S.; Wang, B.; Gong, W.; He, Z.; Xu, Q.; Chen, W.; Zhang, Q.; Zhu, Y.; Yang, J.; Fu, Q.; Chen, C.; Bu, Y.; Gu, L.; Sun, X.; Zhao, H.; Wang, D.; Li, Y., Dual-atom Pt heterogeneous catalyst with excellent catalytic performances for the selective hydrogenation and epoxidation. *Nat. Commun.* **2021,** *12* (1), 3181.

5. Zhang, P.; Hu, Y.; Li, B.; Zhang, Q.; Zhou, C.; Yu, H.; Zhang, X.; Chen, L.; Eichhorn, B.; Zhou, S., Kinetically Stabilized Pd@Pt Core-Shell Octahedral Nanoparticles with Thin Pt Layers for Enhanced Catalytic Hydrogenation Performance. *ACS Catal.* **2015,** *5* (2), 1335-1343.

6. Liu, H.; Yu, H.; Xiong, C.; Zhou, S., Architecture controlled PtNi@$mSiO_2$ and Pt-NiO@$mSiO_2$ mesoporous core-shell nanocatalysts for enhanced *p*-chloronitrobenzene hydrogenation selectivity. *RSC Adv.* **2015,** *5* (26), 20238-20247.

7. Wang, X.; Yu, H.; Hua, D.; Zhou, S., Enhanced Catalytic Hydrogenation Activity and Selectivity of Pt-M_xO_y/Al_2O_3 (M = Ni, Fe, Co) Heteroaggregate Catalysts by *in Situ* Transformation of PtM Alloy Nanoparticles. *J Phys Chem C* **2013,** *117* (14), 7294-7302.

8. Chen, Q.; Jiang, W.; Fan, G., Pt nanoparticles on $Ti_3C_2T_x$-based MXenes as efficient catalysts for the selective hydrogenation of nitroaromatic compounds to amines. *Dalton T* **2020,** *49* (42), 14914-14920.

9. Han, X.; Zhou, R.; Zheng, X.; Jiang, H., Effect of rare earths on the hydrogenation properties of *p*-chloronitrobenzene over polymer-anchored platinum catalysts. *J Mol Catal a-Chem* **2003,** *193* (1-2), 103-108.

10. Han, X.; Chen, Q.; Zhou, R., Study on the hydrogenation of *p*-chloronitrobenzene over carbon nanotubes supported platinum catalysts modified by Mn, Fe, Co, Ni and Cu. *J Mol Catal a-Chem* **2007,** *277* (1-2), 210-214.

11. He, D.; Jiao, X.; Jiang, P.; Wang, J.; Xu, B., An exceptionally active and selective Pt-Au/TiO_2 catalyst for hydrogenation of the nitro group in chloronitrobenzene. *Green Chem.* **2012,** *14* (1), 111-116.

12. Li, J. F.; Ding, S.; Wang, F.; Zhao, H.; Kou, J.; Akram, M.; Xu, M.; Gao, W.; Liu, C.; Yang, H.; Dong, Z., Platinum clusters anchored on sulfur-doped ordered mesoporous carbon for chemoselective hydrogenation of halogenated nitroarenes. *J Colloid Interf Sci* **2022,** *625*, 640-650.

13. Yu, H.; Yu, Z.; Yang, F.; Yan, X.; Yin, H., Enhanced strong metal-support interactions between Pt and WO_{3-x} nanowires for the selective hydrogenation of *p*-chloronitrobenzene. *New J Chem* **2021,** *45* (38), 18065-18069.

14. Chen, H.; He, D.; He, Q.; Jiang, P.; Zhou, G.; Fu, W. S., Selective hydrogenation of *p*-chloronitrobenzene over an Fe promoted Pt/AC catalyst. *RSC Adv.* **2017,** *7* (46), 29143-29148.

15. Gao, M.; Kou, J.; Xu, M.; Yuan, K.; Li, M.; Dong, Z., Electron-rich Pt anchored on covalent triazine

frameworks for the selective hydrogenation of halogenated nitrobenzenes. *Green Chem.* **2024,** *26* (7), 3884-3902.